Laser surface texturing for high friction contacts

Applied Surface Science 357 (2015) 2313–2319

Contents lists available at ScienceDirect

Applied Surface Science

journal homepage: www.elsevier.com/locate/apsusc

Laser surface texturing for high friction contacts

A. Dunn[a,*], K.L. Wlodarczyk[a], J.V. Carstensen[b], E.B. Hansen[b], J. Gabzdyl[c], P.M. Harrison[c], J.D. Shephard[a], D.P. Hand[a]

[a] Institute of Photonics and Quantum Sciences, Heriot-Watt University, Edinburgh EH14 4AS, UK
[b] MAN Diesel & Turbo, Teglholmsgade 41, 2450 Copenhagen SV, Denmark
[c] SPI Lasers UK Ltd, Wellington Park, Tollbar Way, Hedge End, Southampton SO30 2QU, UK

ARTICLE INFO

Article history:
Received 22 July 2015
Received in revised form
24 September 2015
Accepted 28 September 2015
Available online 1 October 2015

Keywords:
Laser surface texturing
High friction
Fibre laser
Static friction
High pressure

ABSTRACT

A pulsed, nanosecond fibre laser with wavelength of 1064 nm was used to texture grade 316 stainless steel and 'low alloy' carbon steel in order to generate contacts with high static friction coefficients. High friction contacts have applications in reducing the tightening force required in joints or to easily secure precision fittings, particularly for larger components where standard methods are difficult and expensive. Friction tests performed at normal pressures of 100 MPa and 50 MPa have shown that very high static friction coefficients greater than 1.25, an increase of 346% over untextured samples at 100 MPa, can be easily achieved by single pass laser texturing of both contacting surfaces with the use of low pulse separations. The high static friction coefficients, obtained at 100 MPa normal pressure with textures with up to 62.5 μm pulse separation (processing speed ~0.67 cm^2/s), were found to be associated with a significant amount of plastic deformation caused by the high normal pressures. As a result, higher normal pressures were found to result in higher friction coefficients.

1. Introduction

Laser surface texturing (LST) is a commonly used surface modification technique with a significant amount of current research focus. Surface modification has many industrial applications due to the number of properties of a material which are surface dependent, such as wettability, corrosion resistance, adhesion and friction. Whilst there are many competing surface modification techniques available, such as electron beam treatment [1,2], chemical treatment [3], plasma treatment [4], electric discharge [5] and sand blasting [6], each of which have their own advantages and disadvantages; LST has several characteristics which are particularly advantageous for certain applications. These include, but are not limited to, the flexibility, repeatability, accuracy, speed, lack of tool wear and negligible effect on the bulk material properties.

Several different techniques have been reported to result in relatively high friction surfaces, although typically the focus is towards increased hardness for wear reduction in these cases. HVOF (high velocity oxygen fuel) and HVAF (high velocity air fuel) spray coatings of WC–10Co4Cr, for example, have been shown to give friction coefficients of around 0.6 at room temperature, and greater than 1 at elevated temperatures of 400 °C [7]. In these tests, coatings were sprayed onto low-carbon Domex 355 steel substrates and tested with Al_2O_3 spheres on a ball on disk tribometer. Electrolytic hard chrome (EHC) plating has also shown promise [8] with friction coefficients of 0.52 ± 0.07 reported at room temperature. Friction tests here were performed with a grade 304 stainless steel ball-on-flat reciprocating tribometer. Some more creative techniques have also been investigated, such as the generation of nano-textures on aluminium substrates by anodic aluminium oxidation [9]. The nano-texture, consisting of a hexagonal array of dimples with ~250 nm diameter, resulted in friction coefficients >4 under dry conditions when measured with a PDMS (polydimethylsiloxane) ball-on-flat test. Each of these techniques have been tested under sliding conditions; as a result, the friction coefficients quoted are kinetic, rather than static as is the focus of the work in this paper, however they give an indication of the coefficients which are achievable.

An interesting idea to intentionally increase the static friction coefficient of a surface has been put forward and tested by Hammerström and Jacobson [10]. By using a combination of photolithography, etching and CVD of diamond, regular arrays of diamond pyramids have been successfully generated with area densities of 2% and 22%. The diamond textures were tested in flat-on-flat tests against both steel and silver substrates at normal pressures up to 20 MPa, with the resulting static friction coefficients

* Corresponding author.
E-mail address: ad134@hw.ac.uk (A. Dunn).

http://dx.doi.org/10.1016/j.apsusc.2015.09.233

consistently >1.2. Such high friction coefficients were obtained due to embedding of the diamond pyramids into the metal substrates, which then require a large force to plough through during the friction tests. Despite the impressive friction coefficients obtained, the intricate and environmentally unfriendly process required to generate such textures make this technique unappealing for industrial processes.

LST has been reported to increase the friction coefficient under sliding conditions [11,12], with increases of up to 100% reported when both mating surfaces have been textured [13], albeit unintentional and undesirable in these cases. More recently, research on purposely increasing the static friction coefficient of a surface has been presented [14], with a focus on textures generated by significant overlapping of pulses, resulting in rough surfaces with a random topography. Increasing the pulse overlap was found to increase the static friction coefficient as well as both the surface roughness and hardness. The preliminary assumption was that the observed increase in friction coefficient is correlated to the hardness increase, with some minor effect from the surface roughness. A second approach has also been considered where raised bumps on the surface are generated by deep penetration welds [15]. In this case, the friction coefficient was found to increase significantly compared to the untextured sample, however the torque-angle curves indicate that this is kinetic friction rather than static friction.

Applications for high static friction surfaces include the reduction of the tightening forces required for a joint or to secure a precision fitting easily [16]. These applications are particularly relevant where the components in question are very large and so are expensive and/or difficult to machine with the required precision. MAN Diesel & Turbo (MDT), for example, are looking for a reliable method of generating high static friction surfaces ($\mu_s > 0.6$) for use in components of large diesel engines.

Following the previous findings [13,14], the work presented in this paper aims to reliably achieve static friction coefficients of greater than 0.6 for applied normal pressures in the range of 50–100 MPa, as required in these types of application, by texturing both of the samples' contacting surfaces with nanosecond pulsed laser radiation.

2. Experimental

2.1. Experimental set-up

Subsequent measurements to [14] suggested that increased energy density (achieved through the reduction of the focal spot size) resulted in higher friction coefficients. As a result, the laser and optics were changed from those used previously in order to obtain the highest energy density possible from the system. Therefore, laser texturing of the samples was performed using a pulsed SPI 20 W EP-S ($M^2 \sim 1.1$) fibre laser with wavelength of 1064 nm, pulse duration of ~220 ns and pulse energy of 0.71 mJ (maximum available, ~167 J/cm^2 compared to ~36 J/cm^2 used in [14]). The laser beam from the fibre was collimated to an 11 mm beam diameter before entering the galvanometric scan head (Raylase RLA1504), which deflects the beam and focusses (~21 μm spot size) it onto the work piece via an F-theta lens (f = 160 mm). Despite the small nominal spot size, the dimensions of the craters formed on the sample surfaces were found to be significantly larger (~60 μm), as previously reported [14]. Both the laser and the scan head are controlled simultaneously by a SCAPS hardware controller and SAMLight computer software, as shown in Fig. 1.

Two different steel alloys were textured for friction testing, commercially available grade 316 stainless steel (SS316) samples and 'low alloy' carbon steel counter parts. The surfaces of both of these parts were finely ground (R_a < 0.4 μm) prior to laser texturing. A

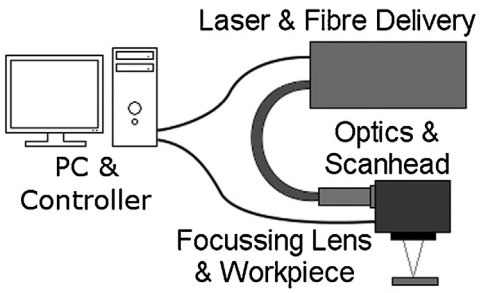

Fig. 1. Schematic of laser processing workstation with the fibre laser and galvo scanner controlled by the PC software and controller.

two dimensional 'hexagonal' arrangement of pulses was used for laser texturing, as shown in Fig. 2, in order to generate a homogeneous surface structure with the aim of achieving a consistent friction coefficient, regardless of the direction of motion.

In order to reduce the parameter space, this layout was used throughout testing with the same pulse separation being used on both sample and counter piece for each individual test. The pulse separation was used as a variable, with the corresponding laser processing parameters calculated as follows:

$$s = \frac{v}{PRF} = \frac{h}{\cos(30^\circ)} \quad (1)$$

where v is the scan speed and PRF is the pulse repetition frequency. A PRF of 20 kHz was used for laser texturing of all samples and all processing was performed in an air atmosphere.

2.2. Testing and measurement

In order to test the friction coefficient of the textured samples, both (opposite) faces of the samples and the two contacting faces of the counter pieces were laser processed. The samples were then mounted in a custom designed testing rig and the normal force was applied through the counter pieces to the sample by two high tensile steel bolts, as shown in Fig. 3. The normal force applied to the sample is directly measured by an in-line load cell (strain gauge) which is monitored whilst manually tightening the bolts to the required level. Normal pressures in the range of 50–100 MPa (corresponding to 20–40 kN) are of interest for several MDT applications and so these values were chosen for friction testing.

After applying the desired normal pressure, the testing rig is moved to a 100 kN hydraulic press (Dartec) which is used to apply the load force (Fig. 3b). It should be noted that the normal pressure is no longer monitored after moving the apparatus to the hydraulic press.

The load force, recorded on a PC along with the 'stroke' distance, applied to the sample is gradually increased until the sample

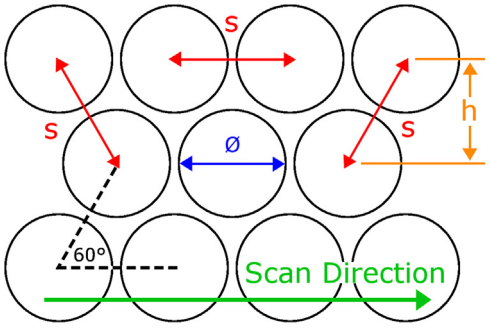

Fig. 2. Schematic of 'hexagonal' laser pulse layout used for high friction texturing; where ϕ is pulse diameter, s is the pulse separation and h is the hatch distance.

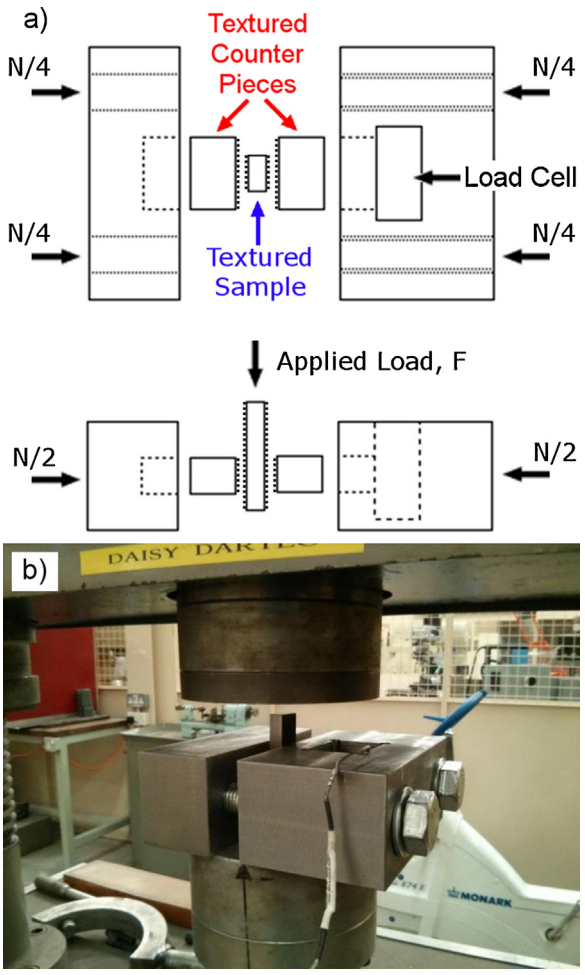

Fig. 3. Schematic of testing rig showing sample, counter pieces and applied forces (*N* denotes normal force) from top-down view (top) and side-on (bottom) views (a) and friction testing set-up on the Dartec hydraulic press with sample held by the normal force, which is applied by the two bolts (b).

exhibits slippage (failure). The force applied at the point of slipping denotes the maximum load force, F_{max}, which is used to calculate the coefficient of static friction, as follows:

$$\mu_s = \frac{F_{max}}{2 \times N} \quad (2)$$

where *N* is the normal force applied to the sample by the bolts. The factor of two relates to the fact that both surfaces of the sample are under test. Upon slipping, the sample was deemed to have 'failed', as a real component would require replacement at this point for the MDT application, and so testing of the samples was stopped at this point. At least five of such tests were performed for each of the sample parameters discussed in this paper, with all tests performed at room temperature.

Analysis of the results and samples was performed by studying the resulting load–extension data, optical microscopy (Leica DM6000M) with depth profiling capabilities and cross-sections of clamped (but untested) samples.

3. Results and discussion

3.1. Standard friction testing

Initial friction tests were performed at a normal pressure of 100 MPa (40 kN). A number of these tests (>5 for each sample parameter) were performed on samples with a range of laser pulse separations from 12.5 μm to 200 μm. Fig. 4 shows a set of typical load against extension curves for these tests.

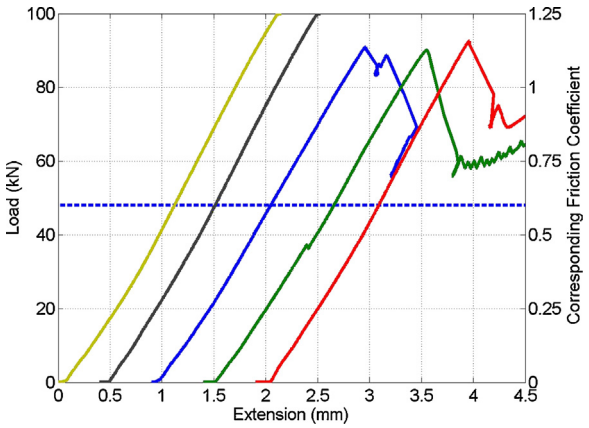

Fig. 4. A typical load–extension plot; 100 MPa normal pressure and 25 μm pulse separation (curves separated for clarity).

As described in Section 2.2, the static friction coefficient is calculated from these plots as the maximum load value prior to slipping (sharp drop in applied load). As can be seen from Fig. 4, several of the tested samples do not exhibit this characteristic slip point below 100 kN. Since the hydraulic press applying the load is limited to 100 kN, the exact slip point, and therefore friction coefficient, for these samples could not be determined. Therefore, the minimum possible friction coefficient of $\mu_s = 1.25$ was taken for these samples. In addition, there is one curve in Fig. 4 which exhibits a very small slip point at around 38 kN load. The consequences of such 'micro-slips' are addressed in Section 3.1.1.

It should also be noted that the response of the sample after the slip point is not of concern, as the contact is deemed to have already failed, i.e. the kinematic friction coefficient is not addressed. Consequently, the application of the load was manually terminated after the sample was known to have slipped, resulting in unusual tails to the load–extension curves.

The friction coefficients were then calculated and averaged for each set of data; both including and excluding the micro-slips, as shown in Fig. 5. The plotted error bars were calculated as the standard deviation of the values for each pulse separation.

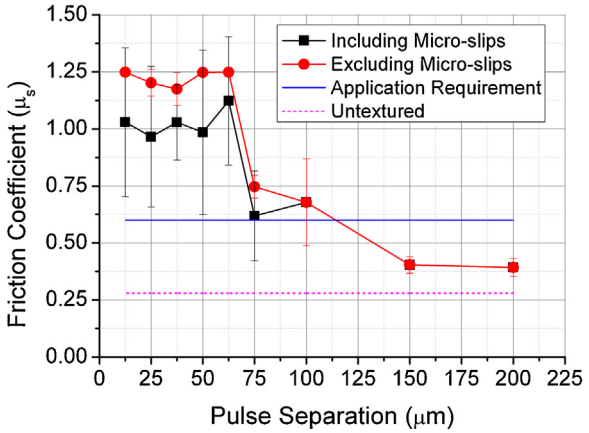

Fig. 5. Dependence of static friction coefficient on laser pulse separation, for coefficients calculated including the observed micro-slips and excluding the micro-slips. The solid and dotted horizontal lines show the minimum coefficient required for the application and the static friction coefficient obtained for untextured samples ($\mu_s = 0.28$, at 100 MPa) respectively, for comparison.

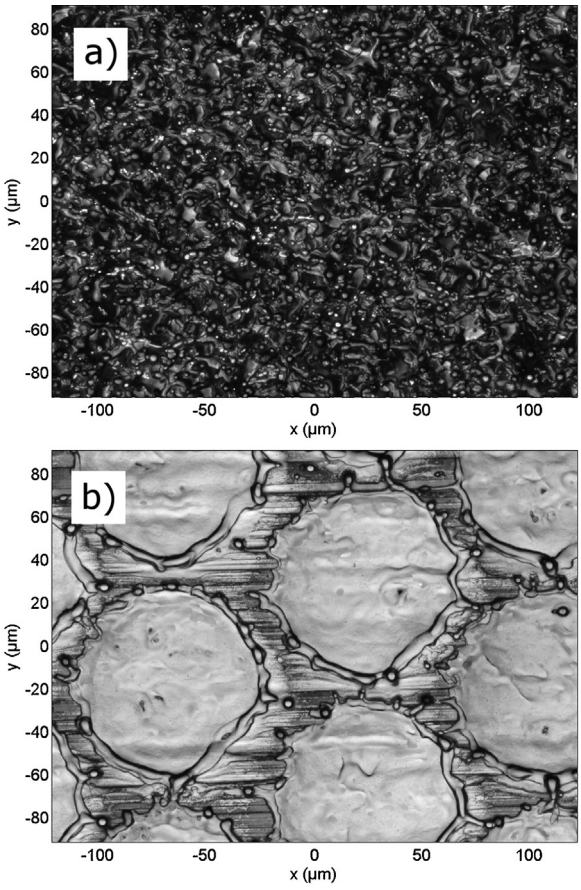

Fig. 6. Optical micrographs of laser textured surfaces with 25 μm pulse separation (a) and 100 μm pulse separation (b) with 0.71 mJ pulses at 20 kHz repetition frequency.

From the results shown in Fig. 5, it can be seen that very high static friction coefficients are obtained with moderate-low pulse separation (<60 μm, >−35% pulse overlap) textures. In this range, friction coefficients of 1.2 or higher are frequently observed when micro-slips are excluded and average values are consistently >0.9 even when the micro-slips are included, albeit with significantly greater variation in the measurements. As pulse separation increases, the observed static friction coefficients decrease dramatically, beginning to converge towards the untextured value at high pulse separation, as expected.

The high friction coefficients seen at low pulse separations are assumed to be the product of good interlocking of the two surface textures, facilitated by plastic deformation caused by the substantial normal pressure. As pulse separation is increased, the number of surface features which can securely interlock decreases, giving a surface which is similar to an untextured surface, resulting in lower friction coefficients.

These assumptions are in agreement with the optical micrographs of the laser textured surfaces, as shown in Fig. 6.

A micrograph of a typical low pulse separation (25 μm) texture is shown in Fig. 6a, with a surface that appears very random and contains a significant number spherical asperities. In comparison, Fig. 6b shows the surface topography of a sample with high pulse separation, 100 μm in this case. Here the hexagonal structure is clearly visible and the number of asperities available for possible interlocking is considerably reduced. Even in this case where the two structures are very dissimilar, the S_a (arithmetic average) roughness values (measured from representative areas of 244 μm × 182 μm) are comparable, as shown in Table 1.

Table 1
Comparison of texturing process rate, friction coefficients and roughness measures for five laser textures, with the two shown in Fig.6 highlighted.

Pulse separation (μm)	Process rate (cm²/s)	Static friction coefficient	S_a (μm)	Peak-trough depth (μm)
12.5	0.03	>1.25	3.68	32.75
25	0.11	>1.20	1.00	10.05
50	0.43	>1.25	0.99	7.14
100	1.72	0.68	0.95	8.84
200	7.14	0.39	0.57	11.61

As pulse separation is decreased, the roughness values increase, however typical roughness measurements do not correspond to the observed difference in friction coefficients.

Analysis using optical microscopy was also performed on a number the tested samples, particularly those which did not slip during testing, such as that shown in Fig. 7.

From Fig. 7a, we can clearly see a significant change in the surface morphology between the region of the texture which has been friction tested (left) and the untested region (right). It was expected that the large normal pressure would cause deformations on the surface of the textured sample – likely reducing the surface roughness in this area. This is clearly visualised in Fig. 7b, where we see a significant decrease in the height of the peaks on the left hand side compared to the right (peak height of ~2.5 μm vs ~5 μm). Area roughness measurements of the two distinct areas were also found to agree with this conclusion, with S_a = 0.71 μm calculated for the tested region compared to S_a = 1.25 μm for the untested region.

Further to the top-down microscopy analysis, cross-sections of the samples after application of the normal load but prior to friction testing were also analysed, shown in Fig. 8.

At 12.5 μm pulse separation, shown in Fig. 8a, the two oxide layers generated by the laser texturing process are deformed significantly by the large normal pressure, resulting in consistent contact

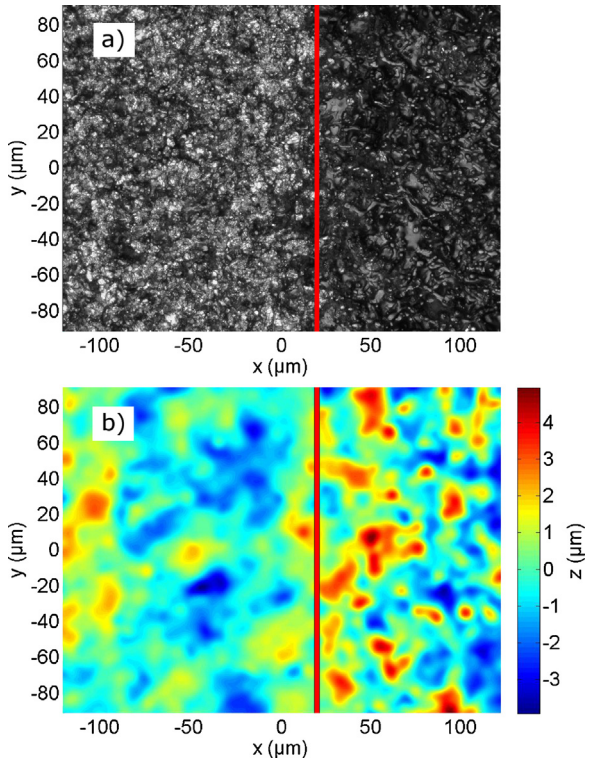

Fig. 7. Optical micrograph (a) and *z*-profile (b) of a sample (37.5 μm pulse separation) after friction testing, with no slipping – tested area on the left of the vertical line and untested on the right.

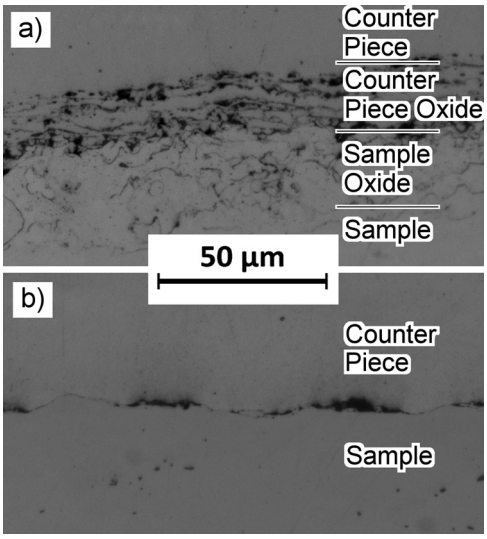

Fig. 8. Cross-sections of two different textures, (a) 12.5 μm pulse separation and (b) 50 μm pulse separation, after application of ~100 MPa normal pressure but without friction testing.

along the interface with very dense interlocking points. The dark spots observable here are small voids generated by the laser texturing process. For the larger pulse separation in Fig. 8b, several deformations are still present however the contact is less consistent (with the presence of observable gaps) in addition to more sparse interlocking points. Despite both of these two textures exhibiting high friction coefficients, it is clear that as pulse separation is increased the interlocking becomes weaker. As a result, the lower coefficients observed at larger pulse separations in Fig. 5 are easily interpreted.

3.1.1. Micro-slips

As noted in Section 3.1 (Fig. 4), several of the load–extension curves show micro-slips. The cause of these slips and the effect they have on the static friction coefficient was initially unclear. As a result, additional tests and observations were made on these samples. Fig. 9 highlights the appearance of the micro-slips and gives a good indication of the scale at which the slip takes place.

The measurements plotted in Fig. 9 show that even after micro-slipping, the load can continue to be increased on some samples without exhibiting any further slippage. Following this, the load was removed from several of these samples and then reapplied as

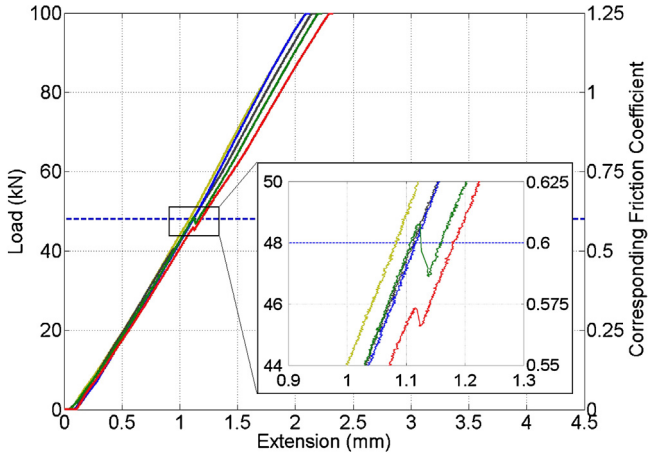

Fig. 9. Load–extension curve for textures with 50 μm pulse separation, with inset highlighting the observed micro-slips.

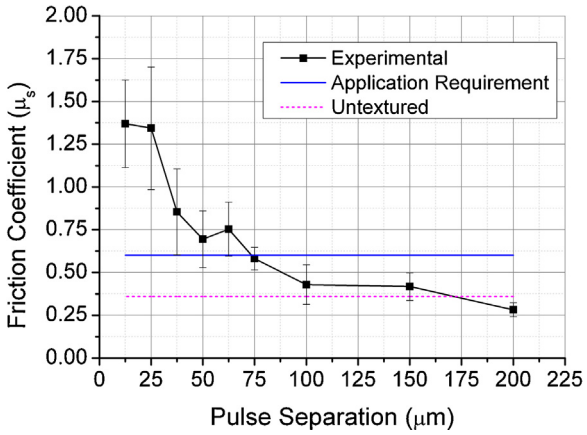

Fig. 10. Dependence of static friction coefficient on laser pulse separation. The solid and dotted horizontal lines show the minimum coefficient required for the application and the static friction coefficient obtained for untextured samples (μ_s = 0.36 at 50 MPa) respectively, for comparison.

in the original friction test. The resulting load–extension curve from these tests showed a straight line as the applied load increased linearly without any slippages. Given this observation, and the small movement of the samples during these micro-slips (<50 μm), it is reasonable to assume that these micro-slips are not representative of the static friction coefficient but rather are very small realignments of the structures, facilitating even better interlocking between them. Therefore, for all following measurements, micro-slips are excluded for the friction coefficient calculations.

3.1.2. Testing at reduced normal pressure (50 MPa)

Since a significant number of friction tests performed with 100 MPa normal pressure exceeded the measurement capabilities of the hydraulic press, textures of the same design were then tested with a lower normal pressure of 50 MPa, thus allowing the determination of friction coefficient values of up to 2.5 with the same testing set-up and equipment. Fig. 10 shows the friction dependence on the pulse separation using 50 MPa normal pressure.

As in Fig. 5, the friction coefficients observed in Fig. 10 are very high, above 1.3 on average with individual measurements as high as 1.9 at low pulse separations (<25 μm). These values decrease sharply as pulse separation is increased and converge towards the untextured baseline value at around 175 μm pulse separation.

Given that the results plotted in Figs. 5 and 10 used identical laser texturing parameters, the measurements can be directly compared as in Fig. 11.

As noted in Section 3.1.2, the overall trends of the curves are very similar for both normal pressures. However, in the range of pulse separation range where the friction coefficients can be resolved at 100 MPa pressure, the samples tested at 100 MPa consistently give higher friction coefficients than those tested at 50 MPa. This implies that the larger normal force causes more plastic deformations of the textured surfaces, allowing better contact and interlocking of the two textures and therefore increased friction coefficients.

3.2. Testing after overloading normal pressure

Given the observed dependence of the static friction coefficient on the applied normal pressure, it was assumed that higher friction coefficients could be achieved by 'overloading' the sample to a very high normal pressure prior to testing at a lower normal pressure. In order to test this, another set of samples were textured and then subjected to a normal pressure of 150 MPa which was then decreased to 50 MPa before testing, without realigning the sample.

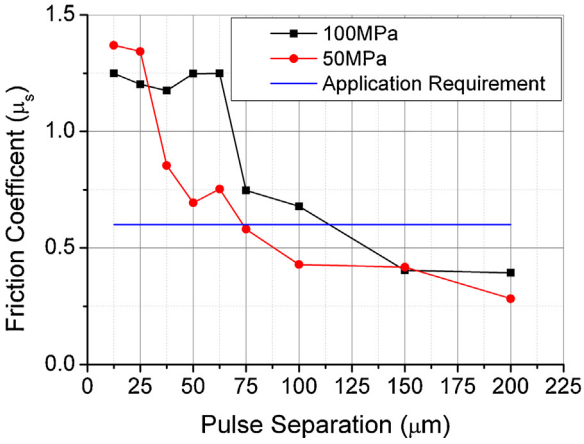

Fig. 11. Comparison of the dependence of static friction coefficients on laser pulse separation for the two applied normal pressures.

Fig. 12 shows the results of these tests in comparison to those already presented in Section 3.1.2.

The measurements shown in Fig. 12 clearly show that by initially applying a very large normal pressure of 150 MPa, extremely high friction coefficients ($\mu_s > 1.5$) can be obtained at lower pulse separations even when testing at much lower normal pressures of 50 MPa. The initial normal pressure of 150 MPa plastically deforms the contacting surfaces significantly more than when only 50 MPa is applied. As a result, even though the pressure is reduced to 50 MPa, there is substantially more interlocking of the two textures than when only 50 MPa is applied, resulting in extremely high static friction coefficients. As discussed in Section 3.1, increasing the pulse separation reduces the ability of the two textures to interlock, due to the low density of features available. Therefore, less plastic deformation takes place and the effectiveness of the high initial normal pressure is reduced. These results are in good agreement with the previous assumptions, based on the original findings, and all but confirm that the high friction coefficients obtained are the result of very good interlocking of the contacting surfaces.

3.3. Testing of polished surfaces

In order to determine whether the observed increase in friction coefficients was related to the increased real contact area, due to the high normal pressure, friction tests were conducted on samples and counter pieces which had their surfaces polished to $R_a < 50$ nm. The load–extension curves for these tests are shown in Fig. 13.

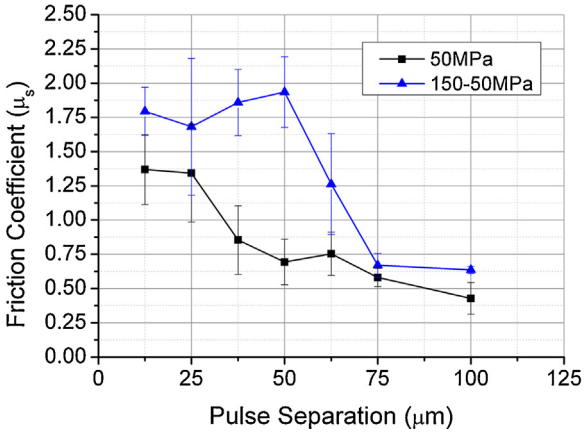

Fig. 12. Comparison of the static friction coefficients obtained at 50 MPa and those loaded to 150 MPa then decreased to 50 MPa prior to friction testing.

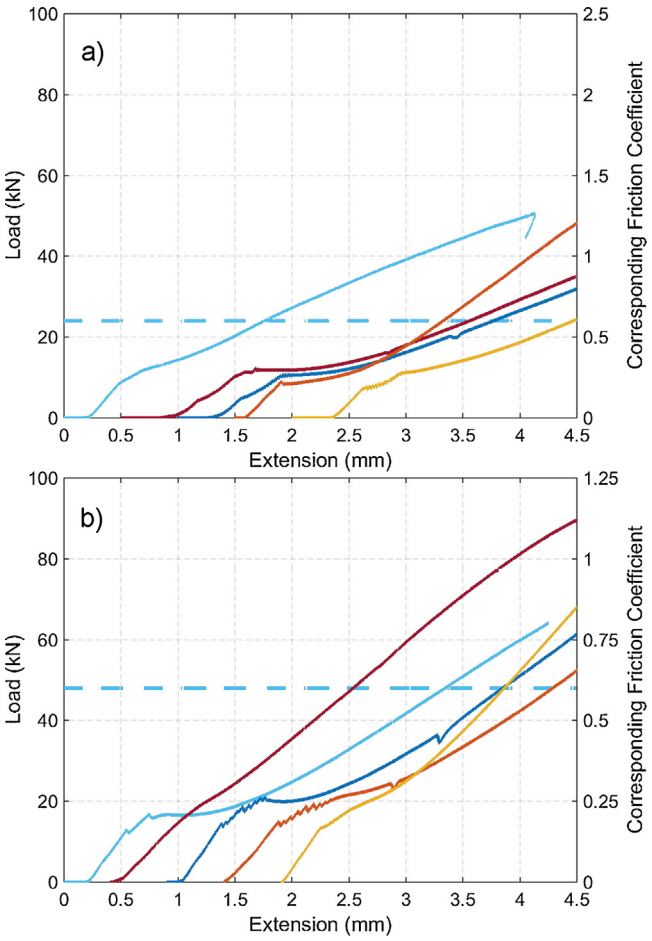

Fig. 13. Load–extension curves for tests performed on polished surfaces at (a) 50 MPa and (b) 100 MPa normal pressures.

Unlike the typical curves shown in Fig. 4, the results presented here do not exhibit the sharp slip point of static friction. Rather, the curves in Fig. 13 show small slip points or continuous sliding, indicative of an adhesion based friction regime for which the static friction coefficient is difficult to determine exactly. However, by considering the change in gradients observed in the load–extension curves in Fig. 13, it is clear that the static friction coefficients are consistently very low ($\mu_s < 0.4$) for both normal pressures. Therefore, the high friction coefficients obtained with the LST samples are primarily obtained by the interlocking features, and associated shearing required for lateral movement, rather than purely increased real contact area.

4. Conclusion

The effect of laser pulse separation and normal pressure was studied in high static friction tests in which both mating surfaces of the contact were identically laser textured. High static friction coefficients $\mu_s > 1.25$ were consistently achieved when using normal pressures of 50 MPa and 100 MPa with pulse separations of less than 60 μm, an increase of 346% over untextured samples at 100 MPa. Significant interlocking of the contacting textures, enabled by plastic deformations due to the large normal pressure, facilitated such large friction coefficients. This is highlighted by the fact that applying a higher normal pressure consistently results in higher friction coefficients than use of lower normal pressure.

Further, intentionally overloading the sample (applying excess normal pressure), before testing at lower normal pressure, gives

higher friction coefficients than when the sample is not overloaded. Tests on polished samples clearly indicate that the large friction increases are not caused by the increased real contact area, but rather the interlocking of features and required shearing of these features for lateral movement of the parts.

The consistently high friction coefficients, in combination with the moderate processing rate (~0.67 cm^2/s, with further optimisation possible) and the other benefits of using lasers for surface modification (flexibility, lack of tool wear, no environmentally unfriendly chemicals, etc.), make LST an industrially appealing for applications requiring surfaces with increased friction.

Acknowledgement

The authors acknowledge the Engineering and Physical Sciences Research Council (EPSRC) for their support of this research (Grant No. EP/J500227/1).

References

[1] R. Nathawat, A. Kumar, N.K. Acharya, Y.K. Vijay, XPS and AFM surface study of PMMA irradiated by electron beam, Surf. Coat. Technol. 203 (2009) 2600–2604.
[2] A. Schulze, M.F. Maitz, R. Zimmermann, B. Marquardt, M. Fischer, C. Werner, M. Went, I. Thomas, Permanent surface modification by electron-beam-induced grafting of hydrophilic polymers to PVDF membranes, RSC Adv. 3 (2013) 22518.
[3] S.E. Elsaka, Influence of chemical surface treatments on adhesion of fiber posts to composite resin core materials, Dental Mater.: Off. Publ. Acad. Dent. Mater. 29 (2013) 550–558.
[4] J.D. Queiroz, A.M. Leal, M. Terada, L.F. Agnez-Lima, I. Costa, N.C. Pinto, S.R. Batistuzzo de Medeiros, Surface modification by argon plasma treatment improves antioxidant defense ability of CHO-k1 cells on titanium surfaces, Toxicology In Vitro: Int. J. Publ. Assoc. BIBRA 28 (2013) 381–387.
[5] A. Moshkovith, V. Perfiliev, D. Gindin, N. Parkansky, R. Boxman, L. Rapoport, Surface texturing using pulsed air arc treatment, Wear 263 (2007) 1467–1469.
[6] S. Beckford, N. Langston, M. Zou, R. Wei, Fabrication of durable hydrophobic surfaces through surface texturing, Appl. Surf. Sci. 257 (2011) 5688–5693.
[7] G. Bolelli, L.M. Berger, T. Börner, H. Koivuluoto, L. Lusvarghi, C. Lyphout, N. Markocsan, V. Matikainen, P. Nylén, P. Sassatelli, R. Trache, P. Vuoristo, Tribology of HVOF- and HVAF-sprayed WC–10Co4Cr hardmetal coatings: a comparative assessment, Surf. Coat. Technol. 265 (2015) 125–144.
[8] W. Fang, T.Y. Cho, J.H. Yoon, K.O. Song, S.K. Hur, S.J. Youn, H.G. Chun, Processing optimization, surface properties and wear behavior of HVOF spraying WC–CrC–Ni coating, J. Mater. Process. Technol. 209 (2009) 3561–3567.
[9] M. Kang, Y.M. Park, B.H. Kim, Y.H. Seo, Micro- and nanoscale surface texturing effects on surface friction, Appl. Surf. Sci. 345 (2015) 344–348.
[10] L. Hammerström, S. Jacobson, Designed high-friction surfaces—influence of roughness and deformation of the counter surface, Wear 264 (2008) 807–814.
[11] L.M. Vilhena, M. Sedlaček, B. Podgornik, J. Vižintin, A. Babnik, J. Možina, Surface texturing by pulsed Nd:YAG laser, Tribol. Int. 42 (2009) 1496–1504.
[12] M. Varenberg, G. Halperin, I. Etsion, Different aspects of the role of wear debris in fretting wear, Wear (2002) 902–910.
[13] I. Etsion, Improving tribological performance of mechanical components by laser surface texturing, Tribol. Lett. 17 (2004) 4.
[14] A. Dunn, J.V. Carstensen, K.L. Wlodarczyk, E.B. Hansen, J. Gabzdyl, P.M. Harrison, J.D. Shephard, D.P. Hand, Nanosecond laser texturing for high friction applications, Opt. Lasers Eng. 62 (2014) 9–16.
[15] J. Schille, F. Ullmann, L. Schneider, M. Graefensteiner, S. Schiefer, M. Gerlach, E. Leidich, H. Exner, Experimental study on laser surface texturing for friction coefficient enhancement, in: International Symposium on Laser Precision Microfabrication, Vilnius, Lithuania, 2014.
[16] J. Gabzdyl, E. Hansen, Surface texturing with ns pulsed fiber lasers, in: NOLAMP, Norwegian University of Science and Technology, Trondheim, Norway, 2011.